Published in final edited form as:
Bioelectromagnetics. 2012 September ; 33(6): 443–451. doi:10.1002/bem.21703.

Inhibition of voltage-gated Na^+ current by nanosecond pulsed electric field (nsPEF) is not mediated by Na^+ influx or Ca^{2+} signaling

Vasyl Nesin and **Andrei G. Pakhomov***
Frank Reidy Research Center for Bioelectrics, Old Dominion University, Norfolk, VA, USA

Abstract

In earlier studies, we found that permeabilization of mammalian cells with nsPEF was accompanied by prolonged inhibition of voltage-gated (VG) currents through the plasma membrane. This study explored if the inhibition of VG Na^+ current (I_{Na}) resulted from (i) reduction of the transmembrane Na^+ gradient due to its influx via nsPEF-opened pores, and/or (ii) downregulation of the VG channels by a Ca^{2+}-dependent mechanism. We found that a single 300 ns electric pulse at 1.6–5.3 kV/cm triggered sustained Na^+ influx in exposed NG108 cells and in primary chromaffin cells, as detected by increased fluorescence of a sodium green dye. In the whole-cell patch clamp configuration, this increase was efficiently buffered by the pipette solution so that the increase in the intracellular concentration of Na^+ ($[Na]_i$) did not exceed 2–3 mM. $[Na]_i$ increased uniformly over the cell volume and showed no additional peaks immediately below the plasma membrane. Concurrently, nsPEF reduced VG I_{Na} by 30–60% (at 4 and 5.3 kV/cm). In control experiments, an even greater increase of Na^+ in the pipette (by 5 mM) did not attenuate VG I_{Na}, thereby indicating that the nsPEF-induced Na^+ influx was not the cause of VG I_{Na} inhibition. Similarly, adding 20 mM of a fast Ca^{2+} chelator 1,2-bis(o-aminophenoxy)ethane-N,N,N',N'-tetraacetic acid (BAPTA) into the pipette solution did not prevent or attenuate the inhibition of the VG I_{Na} by nsPEF. These findings point to possible Ca^{2+}-independent downregulation of the VG Na^+ channels (e.g., caused by alteration of the lipid bilayer) or the direct effect of nsPEF on the channel.

Keywords

electropermeabilization; ion influx; cell membrane; Na channels; patch-clamp

Introduction

Our previous studies found that permeabilization of the cell plasma membrane by intense nsPEFs may be accompanied by prolonged inhibition of voltage-gated (VG) currents through Na^+, Ca^{2+}, and K^+ channels [Pakhomov et al., 2007a,b; Bowman et al., 2008; Nesin et al., 2012]. This previously unknown effect adds to the understanding of nsPEF interactions with living matter and may lead to applications in experimental biology and medicine. However, mechanisms underlying the inhibition of VG currents have not been identified.

At first glance, the most likely and well-expected mechanism is the ion leak current (I_{leak}) through electropores in the plasma membrane. This leak can reduce the transmembrane ion

*Correspondence to: Andrei G. Pakhomov, 4211 Monarch Way, Suite 300 Norfolk, VA 23508, USA. Phone: 210-204-9012, 757-683-8003, andrei@pakhomov.net, apakhomo@odu.edu.

gradient, thereby reducing the driving force for ion flow when VG channels open. This mechanism is purely electrochemical and does not imply any damage or alteration of VG channels or any regulatory biological response. Arguments in favor of this mechanism are its simplicity and the fact that nsPEFs did not cause inhibition of VG currents without a concurrent or preceding increase in I_{leak} (although sometimes the I_{leak} increase was very small and brief). On the other hand, the intracellular ion composition in "patched" cells is strongly buffered by a practically unlimited ion supply from the recording pipette, and it is not clear if I_{leak} can efficiently compete with it to affect any intracellular ion concentration. The central role of the ion gradient reduction is also questioned by the poor correlation between the I_{leak} amplitude and the inhibitory effect, by persistent inhibition of VG currents even after I_{leak} recovery to pre-treatment values, and by the fact that even very modest I_{leak} increases could nonetheless be accompanied by profound suppression of VG Ca^{2+} channel currents [Nesin et al., 2012].

Alternatively, VG currents could be suppressed by an active downregulation of VG channels as a biological response. The activity of VG channels is modulated in multiple ways by cytoplasmic second messengers, cofactors, coupling proteins, phosphorylation, cytosolic Ca^{2+}, membrane tension, cytoskeleton, and membrane lipids [Catterall, 2000, 2010; Hille, 2001; Roberts-Crowley et al., 2009; Suh et al., 2010]. Earlier studies have demonstrated nsPEF-induced intracellular Ca^{2+} bursts in the absence of Ca^{2+} in the bath buffer, presumably due to its release from intracellular stores [White et al., 2004]. Such transient increases in cytosolic Ca^{2+} could potentially mediate the inhibitory modulation of both Ca^{2+} and Na^{+} VG channels [Catterall, 2000; Hille, 2001; Kim et al., 2004; Casini et al., 2009]. Although the pipette buffer contained 5 mM of the Ca^{2+} chelator ethylene glycol tetraacetic acid (EGTA), it was not necessarily sufficient to block intracellular Ca^{2+} signaling [Rispoli et al., 2000; Rossi et al., 2004].

Finally, one cannot exclude that nsPEFs can modify (damage) the structure of VG channels, as proposed for conventional electroporation in a series of studies by Chen and co-authors [Chen and Lee, 1994a,b; Chen et al., 1998, 2006; Chen, 2004, 2005]. By definition, all VG channels are equipped with voltage sensors that are "designed" for a physiological range of membrane potentials, roughly from −100 to +50 mV. One can speculate that the application of extreme supraphysiological transmembrane potentials (500–1,000 mV) could indeed damage or alter the voltage sensor. Although the evidence available to date appears insufficient to prove structural damage to VG channels [Nesin et al., 2012], this mechanism should be considered and further explored.

Our present study was focused on testing the potential role of two mechanisms that could contribute to nsPEF-induced inhibition of VG I_{Na}. Specifically, we (1) quantified the change in the Na^{+} transmembrane gradient due to its influx into nanoporated cells and tested if this change could be responsible for the inhibition, and (2) checked if a high intracellular concentration of a fast Ca^{2+} chelator 1,2-bis(o-aminophenoxy)ethane-N,N,N',N'-tetraacetic acid (BAPTA) would prevent the nsPEF-induced inhibition of VG I_{Na}. In addition, inhibition of VG I_{Na} by nsPEFs that was reported in immortalized NG108 cells is also shown in primary adrenal chromaffin cells.

Materials and Methods

Cell lines

A murine neuroblastoma–rat glioma hybrid cell line (NG108) was obtained from American Type Culture Collection (Manassas, VA) and propagated at 37 °C with 5% CO_2 as described earlier [Nesin et al., 2012]. Some experiments were replicated in a primary culture of bovine adrenal chromaffin cells (a gift from G. L. Craviso, University of Nevada School

of Medicine, Reno, NV). The chromaffin cells were isolated from fresh bovine adrenal medullas and cultured at 1×10^5 cells/ml in Ham's F-12 medium containing 10% (v/v) calf serum, 100 units/ml penicillin, 100 μg/ml streptomycin, 0.25 μg/ml fungizone, and 32 μM cytosine arabinoside. Cell aggregates were dissociated with dispase (Invitrogen, Eugene, OR); for detailed procedures see Hassan et al. [2002] and Craviso [2004]. For nsPEF exposures, cells were transferred onto glass cover slips pre-treated with poly-L-lysine (Sigma-Aldrich, St. Louis, MO) or rat tail collagen, type 1 (Roche Diagnostics, Indianapolis, IN).

Electrophysiology

Whole-cell currents were measured similarly in both cell lines. Detailed procedures have been described in the previous paper [Nesin et al., 2012]. We used an Axopatch 200B amplifier, Digidata 1440A digitizer, and pCLAMP 10 software (Molecular Devices, Foster City, CA). The command voltage was stepped from the holding level of −80 mV to test voltages between −100 mV and +30 mV, with 10 mV increments. The bath buffer was composed of (in mM): 134 NaCl, 10 tetraethylammonium chloride (TEA-Cl), 4 $MgCl_2$, 1 Na-EGTA, 10 *N*-2-hydroxyethylpiperazine-*N'*-2-ethanesulfonic acid (HEPES), and 5 glucose (pH 7.4). The recording pipette was filled with (in mM): 139 CsCl, 1 NaCl, 3 $MgCl_2$, 5 Cs-EGTA, 10 HEPES, and 1 Mg-ATP (pH 7.2). In some experiments, the concentration of Na^+ in the pipette was increased while the content of Cs^+ was decreased by the same amount. For fluorescent measurements of Na^+ uptake, the pipette buffer was supplemented with 1 μM of Sodium Green dye (Invitrogen).

For experiments with BAPTA, the pipette buffer contained (in mM): 115 CsCl, 1 NaCl, 20 Cs-BAPTA, 5 $CaCl_2$, 3 $MgCl_2$, 10 HEPES, and 1 Mg-ATP (pH 7.2). The free Ca^{2+} concentration in this buffer was about 50 nM, as computed with a Webmaxc Extended calculator (http://maxchelator.stanford.edu).

The membrane potentials reported below have not been corrected for junction potentials (about 5 mV). The osmolality of all solutions was between 290 and 310 mOsm/kg as measured with a freezing point microosmometer (Advanced Instruments, Norwood, MA). The chemicals were purchased from Sigma-Aldrich.

Exposure to nsPEFs and local E-field modeling

General exposure procedures, nsPEF measurements, and E-field simulation were the same as described recently [Bowman et al., 2010; Pakhomova et al., 2011; Nesin et al., 2012]. Nearly rectangular 300 ns pulses were delivered to an individual patched cell with a pair of tungsten rod electrodes (80–100 μm diameter, 120–200 μm gap), which were tapered to 7–10 μm over the last 260 μm of their length. Using a robotic micromanipulator (MPC-325, Sutter Instrument, Novato, CA), the electrodes were positioned precisely at 50 μm above the coverslip surface so that the selected cell was in the middle of the gap between their tips; the patch-clamp recording pipette was attached to the cell at about a 90° angle to the line between the tips. All exposures were performed at room temperature (23–24 °C). Within each series of experiments, sham exposures and nsPEF treatments were carefully randomized.

Cell imaging

Sodium Green, a visible light-excitable Na^+ indicator (exc/em 492/517 nm), entered patched cells by passive diffusion from the recording pipette. A continual exchange of the dye with the pipette ensured constant dye concentration in the cell throughout the experiment, without any noticeable bleaching. The dye was excited using a Lambda DG-4 illuminator (Sutter). The emission signal was recorded with a C9100-02 electron multiplier CCD camera

(Hamamatsu, Bridgewater, NJ) controlled with MetaFluor software (Molecular Devices). Fluorescent images were typically taken every 2 s throughout the duration of the experiment and quantified off-line with MetaFluor.

In a special series of experiments, the intensity of the dye fluorescence was calibrated against the Na^+ concentration in the pipette buffer (from 1 to 20 mM). Cells were patched in a usual manner and imaged using the same acquisition parameters as in experiments with nsPEFs. The emission of the dye was averaged over the cell body area, but excluding any cellular processes. Within the range of interest, the dye emission increased linearly with Na^+ concentration (data not shown).

Results

Inhibition of I_{Na} and Na^+ influx into nsPEF-exposed cells

A typical timeline of the experiment is presented in Figure 1. At a certain point after the whole-cell recording configuration was formed (usually within 1–2 min), we began taking fluorescent images of the cell (every 2 s). At 20 s prior to nsPEF exposure, membrane currents were tested by applying a voltage-step protocol as described above. Next, the nsPEF-delivering electrodes were lowered to a predefined “work” position using the automatic targeting function of the micromanipulator. A single 300 ns electric pulse was delivered at 0 s, and the electrodes were withdrawn immediately afterward (if the electrodes were left in the bath buffer, they could increase the line frequency (60 Hz) interference and cause zero-voltage shifts during the following patch-clamp measurements). The membrane currents were probed again with the same voltage-step protocol 20 and 30 s after the nsPEF exposure. I_{Na} was isolated from I_{leak} off-line using the method described recently [Nesin et al., 2012].

As seen in Figure 1, nsPEFs caused an immediate influx of Na^+ into the cell, profoundly increased I_{leak}, and decreased VG I_{Na}. Notably, I_{leak} showed partial recovery 30 s after the exposure, whereas I_{Na} remained inhibited.

Na^+ uptake by exposed NG108 and chromaffin cells as a function of the E-field and time after exposure is presented in Figure 2. The initial $[Na]_i$ in patched cells was at the equilibrium with the pipette buffer (1 mM), whereas the extracellular buffer contained 135 mM Na^+. In both cell lines, nsPEF triggered an immediate Na^+ influx, proportional to the amplitude of the applied pulse. However, even with the highest tested E-field of 5.3 kV/cm, $[Na]_i$ increased rather modestly, to a maximum of about 3 mM. Hence, Na^+ diffusion from the pipette was sufficient to counter the Na^+ influx through the electroporated plasma membrane and to keep $[Na]_i$ low, just slightly above its concentration in the pipette.

Membrane currents in the same cells measured before and 20 s after the exposure are presented in Figure 3 A and B. The nsPEF at 2.7 kV/cm significantly increased I_{leak} in both NG108 and chromaffin cells, and increasing the E-field to 4 kV/cm also caused the inhibition of I_{Na}. In the right panel of the Figure 3A (5.3 kV/cm), the portion of the current-voltage (I-V) curve that corresponded to the maximum activation of VG Na^+ channels (above 0 mV) was fitted with a linear function. The intercept of the best fit line with the abscissa (which corresponds to the equilibrium potentials for Na^+) was at 115 mV for control cells and 83 mV for exposed cells. Based on the Nernst equation for ion equilibrium, these values corresponded to 1.5 mM of $[Na]_i$ for control cells and 5 mM of $[Na]_I$ for exposed cells (with 135 mM Na in the bath buffer). Given the inaccuracy of the linear fit, the inherent variability between cells, and the less than 100% ion selectivity of VG Na^+ channels, these data are in a remarkable agreement with the measurements of Sodium Green emission (Fig. 2).

Next, we tested if the increase in $[Na]_i$ from 1 to 6 mM (simply by using different pipette buffers) would cause an inhibition of VG I_{Na} (Fig. 3C). The data show that such change had no effect on the amplitude of I_{Na} or the shape of the I-V curve, other than the expected shift of the equilibrium potential toward zero when the internal Na^+ concentration was increased.

Overall, these experiments confirmed that nsPEFs triggered a significant Na^+ influx, but the respective change in the $[Na]_i$ was too modest to be responsible for the inhibition of VG I_{Na} (at least in cells that were "patched" prior to exposure so that the internal Na^+ was buffered by the pipette solution). Nonetheless, one could speculate that $[Na]_i$ increased just in the immediate vicinity of the plasma membrane, with progressive dilution when going further into the cell and/or closer to the tip of the pipette. Such local increases in Na^+ would be missed by fluorescence measurements of the whole cell but can be resolved by regional measurements, e.g., along a line drawn over the cell body in the direction between two nsPEF-delivering electrodes (Fig. 4).

In the illustrated experiment, the emission intensity measured along the dashed line remained constant prior to nsPEF exposure. The emission was maximum over the center of the cell body and gradually tapered toward the edges, apparently following the thickness of the cell. Immediately after application of a 300 ns pulse at 5.3 kV/cm the emission started to grow, indicating an increase in the Na^+ concentration. This increase, however, was gradual from the cell edges to its center and did not show any discernible Na^+ increase immediately under the cell membrane. Apparently, Na^+ diffusion within the cell was fast and efficient enough to prevent excessive Na^+ accumulation at any location.

Effect of internal Ca^{2+} buffering with BAPTA

According to the supplier (Invitrogen), BAPTA is more selective for Ca^{2+} than EGTA and binds Ca^{2+} ions 50–400 times faster. Therefore, BAPTA can inhibit Ca^{2+} transients that are not necessarily fully blocked by EGTA, especially at a lower concentration. In addition, the BAPTA-based pipette solution was supplemented with 5 mM Ca^{2+} to buffer free intracellular Ca^{2+} at about 50 nM. This value is at least 10 times higher than that estimated for the EGTA-based solution (which did not have any purposely added Ca^{2+}). The idea pursued here was that the already increased free Ca^{2+} background will make any nsPEF-induced Ca^{2+} transients even more inconsequential.

In Figure 5, the induction of I_{leak} and the inhibition of I_{Na} by nsPEFs are compared for the EGTA- and BAPTA-based pipette solutions. To minimize variability between individual cells, the current traces recorded 20 s prior to the exposure were subtracted from the current traces that were recorded in the same cell 30 s after the exposure; the resulting difference reflects the change caused by the nsPEF. The averaged data were also compared to the effects of sham exposure for each of the tested pipette solutions.

Sham-exposed cells displayed a minor reduction in the VG I_{Na} (presumably due to cell rundown with time) and no changes in I_{leak}. The cells exposed to a 300 ns pulse at 4 kV/cm developed a larger I_{leak} and showed a significantly greater reduction of I_{Na}. The presence of 20 mM BAPTA concurrently with elevating free internal Ca^{2+} to 50 nM did not prevent the inhibition of VG I_{Na} and had no significant effect on the amplitude of I_{leak}.

Discussion

This study confirmed the ability of nsPEFs to inhibit VG I_{Na} and, for the first time, extended this result to primary cells. Within studied limits, nsPEF effects in NG108 cells and bovine adrenal chromaffin cells were qualitatively the same.

We have quantified the $[Na]_i$ increase in nsPEF-exposed cells and found that it was too small to account for the reduction of VG I_{Na} by a trivial reduction of the Na^+ electrochemical gradient. Likewise, intracellular Ca^{2+} transients that could potentially be elicited by nsPEFs apparently played no role in the nsPEF-induced inhibition of VG I_{Na}. We can now conclude that the inhibition of VG I_{Na} was caused by Ca^{2+}-independent signaling pathways or by alterations of the channel itself.

The lipid bilayer of the cell plasma membrane is the primary target of the externally applied electric field. In addition to the merely structural function of the membrane, its regulatory lipids (in particular, phosphatidylinositol (4,5)-bisphosphate, PIP_2, and phosphatidylinositol (3,4,5)-trisphosphate, PIP_3) are intimately involved in the modulation of multiple types of ion channels [Gamper and Shapiro, 2007; Suh and Hille, 2008; Roberts-Crowley et al., 2009; Suh et al., 2010]. It is tempting to hypothesize that PIP_2 can be depleted from the inner leaflet of the membrane by its externalization through nsPEF-opened lipidic pores (similar to what was shown for phosphatidylserine [Vernier et al., 2003, 2004, 2006; Pakhomov et al., 2009; Pakhomov and Pakhomova, 2010]). PIP_2 depletion can be responsible for the nsPEF-induced inhibition of VG Ca^{2+} channels [Nesin et al., 2012]; however, VG Na^+ channels do not appear sensitive to PIP_2 [Hilgemann et al., 2001]. Nonetheless, disruption of the phospholipid bilayer by nsPEFs appears a critical step for subsequent inhibition of VG channels, although exact links between these events have yet to be identified.

While the altered electrochemical balance of Na^+ has been found to play a small role in the inhibition of VG channels, it is important to note that all our measurements were performed in patched cells. In the whole-cell patch-clamp recording configuration, $[Na]_i$ is buffered by the pipette solution, which offsets the Na^+ influx through electropores. In intact (not patched) cells exposed to nsPEFs, the increase in $[Na]_i$ will likely be greater, and the resulting reduction in the Na^+ transmembrane gradient may become an additional factor contributing to the inhibition of VG I_{Na}.

Direct damage to VG channels, as suggested by Chen and co-authors for long (4 ms) electric pulses [Chen, 2004, 2005; Chen et al., 2006], is another potential mechanism of the nsPEF effect that needs investigation. Experiments using VG channels embedded in artificial bilayer membranes, as well as structural analyses and biochemical assays sensitive to protein conformation will likely be the tools needed to verify this mechanism.

Aside from mechanistic studies, further research may focus on implications of the inhibition of VG channels for cell and tissue function. As expected, application of nsPEFs may lower excitability in nerve and muscle cells and block nerve conduction. In addition to these well-known roles of VG Na^+ channels in excitable cells, there is growing evidence of their upregulation in cancer cells and important roles in cell adhesion, migration, invasiveness, and angiogenesis [Grimes et al., 1995; Fraser et al., 2005; Fiske et al., 2006; Roger et al., 2006; Onkal and Djamgoz, 2009; Shao et al., 2009; Andrikopoulos et al., 2011]. Hence, one can anticipate that the inhibition of VG I_{Na} could be an added benefit of the developing therapies that employ nsPEFs for tumor ablation.

Acknowledgments

Grant Sponsors: National Cancer Institute, Grant number: R01CA125482; National Institute of General Medical Sciences, Grant number: R01GM088303; Air Force Office of Scientific Research, Grant number: LRIR 09RH09COR.

The authors thank G. L. Craviso for a kind gift of primary bovine chromaffin cells and instructions on handling them. We also thank G. P. Tolstykh for ideas and fruitful discussion regarding possible role of phosphoinositides in cellular effects of nsPEF.

References

Andrikopoulos P, Fraser SP, Patterson L, Ahmad Z, Burcu H, Ottaviani D, Diss JK, Box C, Eccles SA, Djamgoz MB. Angiogenic functions of voltage-gated Na+ channels in human endothelial cells: Modulation of vascular endothelial growth factor (VEGF) signaling. J Biol Chem. 2011; 286:16846–16860. [PubMed: 21385874]

Bowman, A.; Xiao, S.; Schoenbach, KS.; Pakhomov, AG. Inhibition of voltage-gated calcium channels of cell plasma membrane by nanosecond electric pulses. Bioelectromagnetics Society's 30th Annual Meeting; June 8–12, 2008; San Diego, CA. 2008. p. 75-76.

Bowman AM, Nesin OM, Pakhomova ON, Pakhomov AG. Analysis of plasma membrane integrity by fluorescent detection of Tl^+ uptake. J Membr Biol. 2010; 236:15–26. [PubMed: 20623351]

Casini S, Verkerk AO, van Borren MM, van Ginneken AC, Veldkamp MW, de Bakker JM, Tan HL. Intracellular calcium modulation of voltage-gated sodium channels in ventricular myocytes. Cardiovasc Res. 2009; 81:72–81. [PubMed: 18829699]

Catterall WA. Structure and regulation of voltage-gated Ca^{2+} channels. Annu Rev Cell Dev Biol. 2000; 16:521–555. [PubMed: 11031246]

Catterall WA. Signaling complexes of voltage-gated sodium and calcium channels. Neurosci Lett. 2010; 486:107–116. [PubMed: 20816922]

Chen W. Supra-physiological membrane potential induced conformational changes in K+ channel conducting system of skeletal muscle fibers. Bioelectrochemistry. 2004; 62:47–56. [PubMed: 14990325]

Chen W. Electroconformational denaturation of membrane proteins. Ann N Y Acad Sci. 2005; 1066:92–105. [PubMed: 16533921]

Chen W, Han Y, Chen Y, Astumian D. Electric field-induced functional reductions in the K^+ channels mainly resulted from supramembrane potential-mediated electroconformational changes. Biophys J. 1998; 75:196–206. [PubMed: 9649379]

Chen W, Lee RC. Altered ion channel conductance and ionic selectivity induced by large imposed membrane potential pulse. Biophys J. 1994a; 67:603–612. [PubMed: 7948676]

Chen W, Lee RC. Evidence for electrical shock-induced conformational damage of voltage-gated ionic channels. Ann N Y Acad Sci. 1994b; 720:124–135. [PubMed: 8010631]

Chen W, Zhongsheng Z, Lee RC. Supramembrane potential-induced electroconformational changes in sodium channel proteins: A potential mechanism involved in electric injury. Burns. 2006; 32:52–59. [PubMed: 16384650]

Craviso GL. Generation of functionally competent single bovine adrenal chromaffin cells from cell aggregates using the neutral protease dispase. J Neurosci Methods. 2004; 137:275–281. [PubMed: 15262071]

Fiske JL, Fomin VP, Brown ML, Duncan RL, Sikes RA. Voltage-sensitive ion channels and cancer. Cancer Metastasis Rev. 2006; 25:493–500. [PubMed: 17111226]

Fraser SP, Diss JK, Chioni AM, Mycielska ME, Pan H, Yamaci RF, Pani F, Siwy Z, Krasowska M, Grzywna Z, Brackenbury WJ, Theodorou D, Koyutürk M, Kaya H, Battaloglu E, De Bella MT, Slade MJ, Tolhurst R, Palmieri C, Jiang J, Latchman DS, Coombes RC, Djamgoz MBA. Voltage-gated sodium channel expression and potentiation of human breast cancer metastasis. Clin Cancer Res. 2005; 11:5381–5389. [PubMed: 16061851]

Gamper N, Shapiro MS. Regulation of ion transport proteins by membrane phosphoinositides. Nat Rev Neurosci. 2007; 8:921–934. [PubMed: 17971783]

Grimes JA, Fraser SP, Stephens GJ, Downing JE, Laniado ME, Foster CS, Abel PD, Djamgoz MB. Differential expression of voltage-activated Na+ currents in two prostatic tumour cell lines: Contribution to invasiveness in vitro. FEBS Lett. 1995; 369:290–294. [PubMed: 7649275]

Hassan N, Chatterjee I, Publicover NG, Craviso GL. Mapping membrane-potential perturbations of chromaffin cells exposed to electric fields. IEEE Transactions on Plasma Science. 2002; 30:1516–1524.

Hilgemann DW, Feng S, Nasuhoglu C. The complex and intriguing lives of PIP_2 with ion channels and transporters. Sci STKE. 2001:re19. 2001. [PubMed: 11734659]

Hille, B. Ionic channels of excitable membranes. Sunderland, MA: Sinauer Associates; 2001.

Kim J, Ghosh S, Liu H, Tateyama M, Kass RS, Pitt GS. Calmodulin mediates Ca^{2+} sensitivity of sodium channels. J Biol Chem. 2004; 279:45004–45012. [PubMed: 15316014]

Nesin V, Bowman AM, Xiao S, Pakhomov AG. Cell permeabilization and inhibition of voltage-gated Ca^{2+} and Na^{+} channel currents by nanosecond pulsed electric field (nsPEF). Bioelectromagnetics. 2012 (in press).

Onkal R, Djamgoz MB. Molecular pharmacology of voltage-gated sodium channel expression in metastatic disease: Clinical potential of neonatal Nav1.5 in breast cancer. Eur J Pharmacol. 2009; 625:206–219. [PubMed: 19835862]

Pakhomov AG, Bowman AM, Ibey BL, Andre FM, Pakhomova ON, Schoenbach KH. Lipid nanopores can form a stable, ion channel-like conduction pathway in cell membrane. Biochem Biophys Res Commun. 2009; 385:181–186. [PubMed: 19450553]

Pakhomov, AG.; Kolb, J.; White, J.; Shevin, R.; Pakhomova, ON.; Schoenbach, KS. Membrane effects of ultrashort (nanosecond) electric stimuli. Society for Neuroscience 37th Annual Meeting; Nov. 2–7, 2007; San Diego, CA. 2007a. 2007 Neuroscience Meeting Planner CD-ROM, Presentation Number: 317.14.

Pakhomov, AG.; Pakhomova, ON. Nanopores: A distinct transmembrane passageway in electroporated cells. In: Pakhomov, AG.; Miklavcic, D.; Markov, MS., editors. Advanced Electroporation Techniques in Biology in Medicine. Boca Raton: CRC Press; 2010. p. 178-194.

Pakhomov, AG.; White, J.; Shevin, R.; Kolb, J.; Schoenbach, KS. Bioeffects of extremely high peak power, ultra-short electric field pulses. Malaysia: Kuala Lumpur; 2007b. p. 20-23.http://radiology.um.edu.my/emf2007/emf-2007-proceedings.pdf

Pakhomova ON, Gregory BW, Khorokhorina VA, Bowman AM, Xiao S, Pakhomov AG. Electroporation-induced electrosensitization. PLoS One. 2011; 6:e17100. [PubMed: 21347394]

Rispoli G, Martini M, Rossi ML, Rubbini G, Fesce R. Ca2+-dependent kinetics of hair cell Ca2+ currents resolved with the use of cesium BAPTA. Neuroreport. 2000; 11:2769–2774. [PubMed: 10976960]

Roberts-Crowley ML, Mitra-Ganguli T, Liu L, Rittenhouse AR. Regulation of voltage-gated Ca2+ channels by lipids. Cell Calcium. 2009; 45:589–601. [PubMed: 19419761]

Roger S, Potier M, Vandier C, Besson P, Le Guennec JY. Voltage-gated sodium channels: New targets in cancer therapy? Curr Pharm Des. 2006; 12:3681–3695. [PubMed: 17073667]

Rossi ML, Martini M, Rispoli G, Farinelli F, Fesce R. Intracellular Ca2+ buffers can dramatically affect Ca2+ conductances in hair cells. Hearing Res. 2004; 195:67–74.

Shao D, Okuse K, Djamgoz MB. Protein-protein interactions involving voltage-gated sodium channels: Post-translational regulation, intracellular trafficking and functional expression. Int J Biochem Cell Biol. 2009; 41:1471–1481. [PubMed: 19401147]

Suh BC, Hille B. PIP_2 is a necessary cofactor for ion channel function: How and why? Annu Rev Biophys. 2008; 37:175–195. [PubMed: 18573078]

Suh BC, Leal K, Hille B. Modulation of high-voltage activated Ca(2+) channels by membrane phosphatidylinositol 4,5-bisphosphate. Neuron. 2010; 67:224–238. [PubMed: 20670831]

Vernier PT, Li A, Marcu L, Craft CM, Gundersen MA. Ultrashort pulsed electric fields induce membrane phospholipid translocation and caspase activation: Differential sensitivities of Jurkat T lymphoblasts and rat glioma C6 cells. IEEE Transactions on Dielectrics and Electrical Insulation. 2003; 10:795–809.

Vernier PT, Sun Y, Marcu L, Craft CM, Gundersen MA. Nanoelectropulse-induced phosphatidylserine translocation. Biophys J. 2004; 86:4040–4048. [PubMed: 15189899]

Vernier PT, Ziegler MJ, Sun Y, Gundersen MA, Tieleman DP. Nanopore-facilitated, voltage-driven phosphatidylserine translocation in lipid bilayers–in cells and in silico. Phys Biol. 2006; 3:233–247. [PubMed: 17200599]

White JA, Blackmore PF, Schoenbach KH, Beebe SJ. Stimulation of capacitative calcium entry in HL-60 cells by nanosecond pulsed electric fields. J Biol Chem. 2004; 279:22964–22972. [PubMed: 15026420]

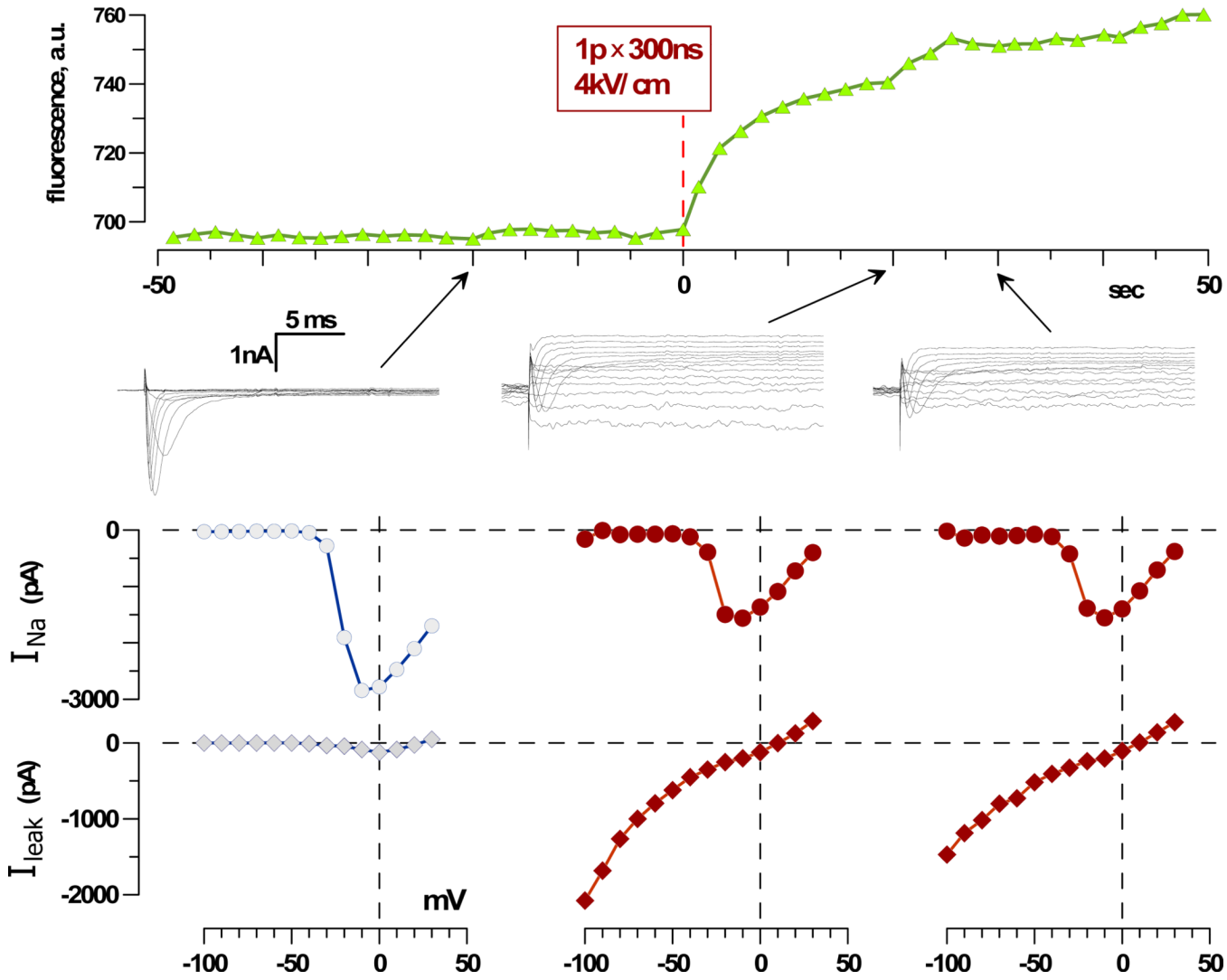

Fig. 1.

Timeline of the experiment and typical effects of nsPEF in a chromaffin cell. **Top:** Cell images were taken and quantified repeatedly before and after the delivery of one 300 ns pulse at 4 kV/cm at 0 s (dashed line). **Center:** Whole-cell currents in response to voltage steps from −100 mV to +30 mV, in 10-mV increments, as measured 20 s before exposure and 20 and 30 s after (arrows). The membrane potential was stepped from the holding value of −80 mV to voltages from −100 mV to +30 mV, in 10-mV increments. **Bottom:** Respective current-voltage (I-V) curves for the fast-inactivating current (VG I_{Na}) and non-inactivating current (I_{leak}). This is a representative experiment out of 12; mean data are shown in Figures 2 and 3.

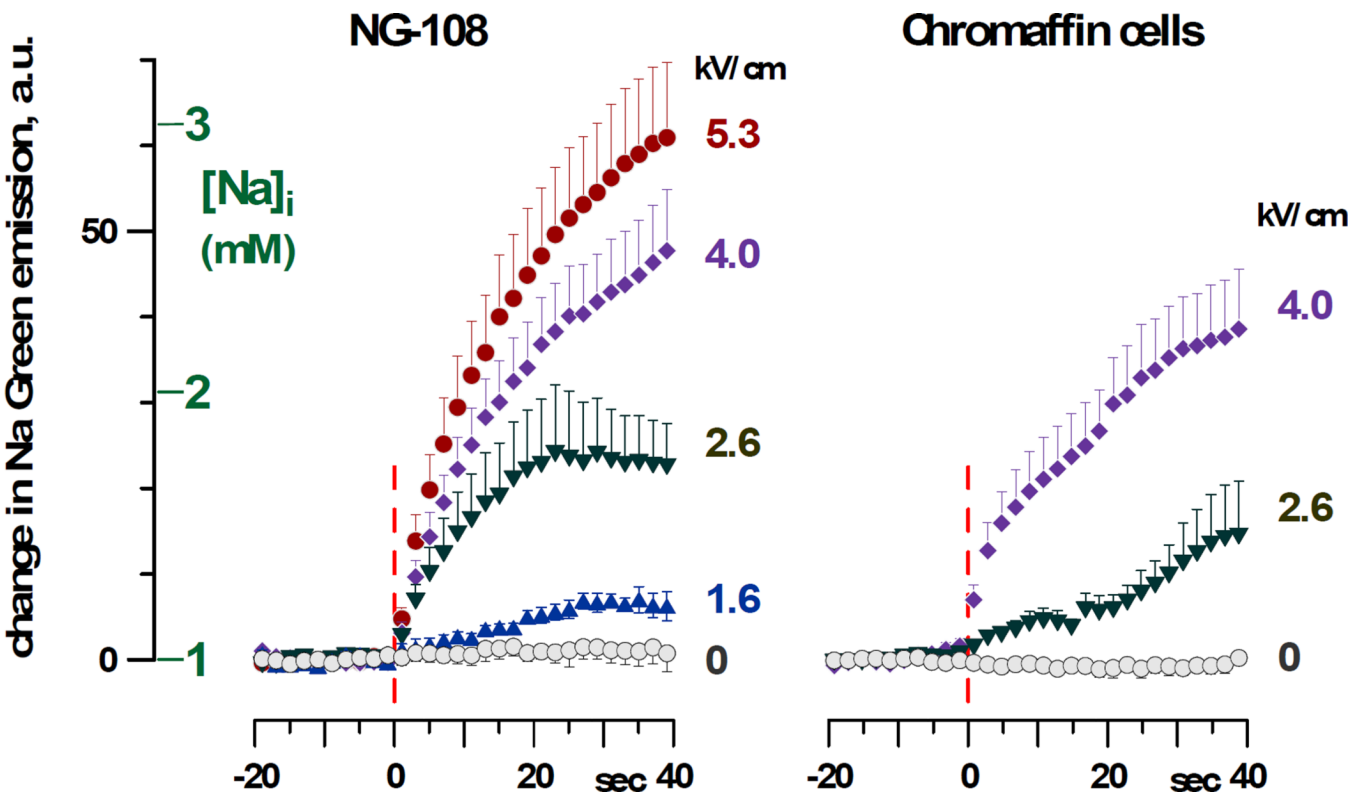

Fig. 2.

Increase in Sodium Green fluorescence and respective change in $[Na]_i$ triggered by nsPEF exposure in NG108 cells and adrenal chromaffin cells. Fluorescence was quantified as an average value within a contour of the cell body. Cells were exposed at 0 s (vertical dashed lines) to one 300 ns pulse at the indicated E-field amplitude. Mean values ± s.e. for 5–12 experiments per group; for clarity, error bars are drawn in one direction only. See Figure 3A and B for concurrent measurements of membrane currents in these cells.

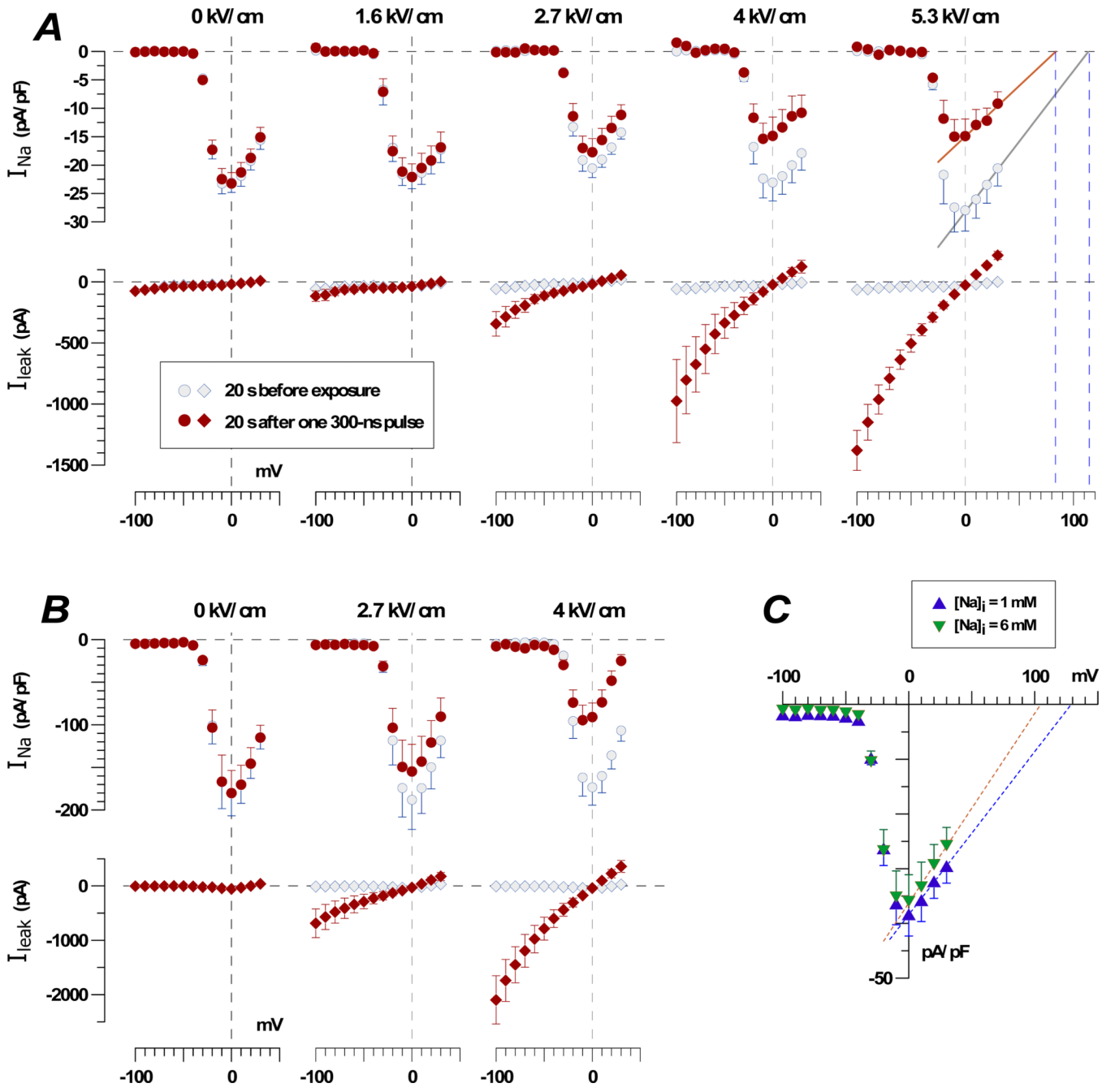

Fig. 3.

Effect of nsPEF and increasing Na^+ concentration in the pipette buffer on membrane currents in NG108 cells (**A** and **C**) and adrenal chromaffin cells (**B**). **A** and **B:** Currents were measured 20 s prior to one 300 ns pulse at the indicated E-field amplitude and 20 s after. Note the E-field-dependent enhancement of I_{leak} and inhibition of the VG I_{Na} in both cell lines. **C:** VG I_{Na} was measured 1–2 min after forming the whole-cell patch clamp recording configuration, without any nsPEF exposure.

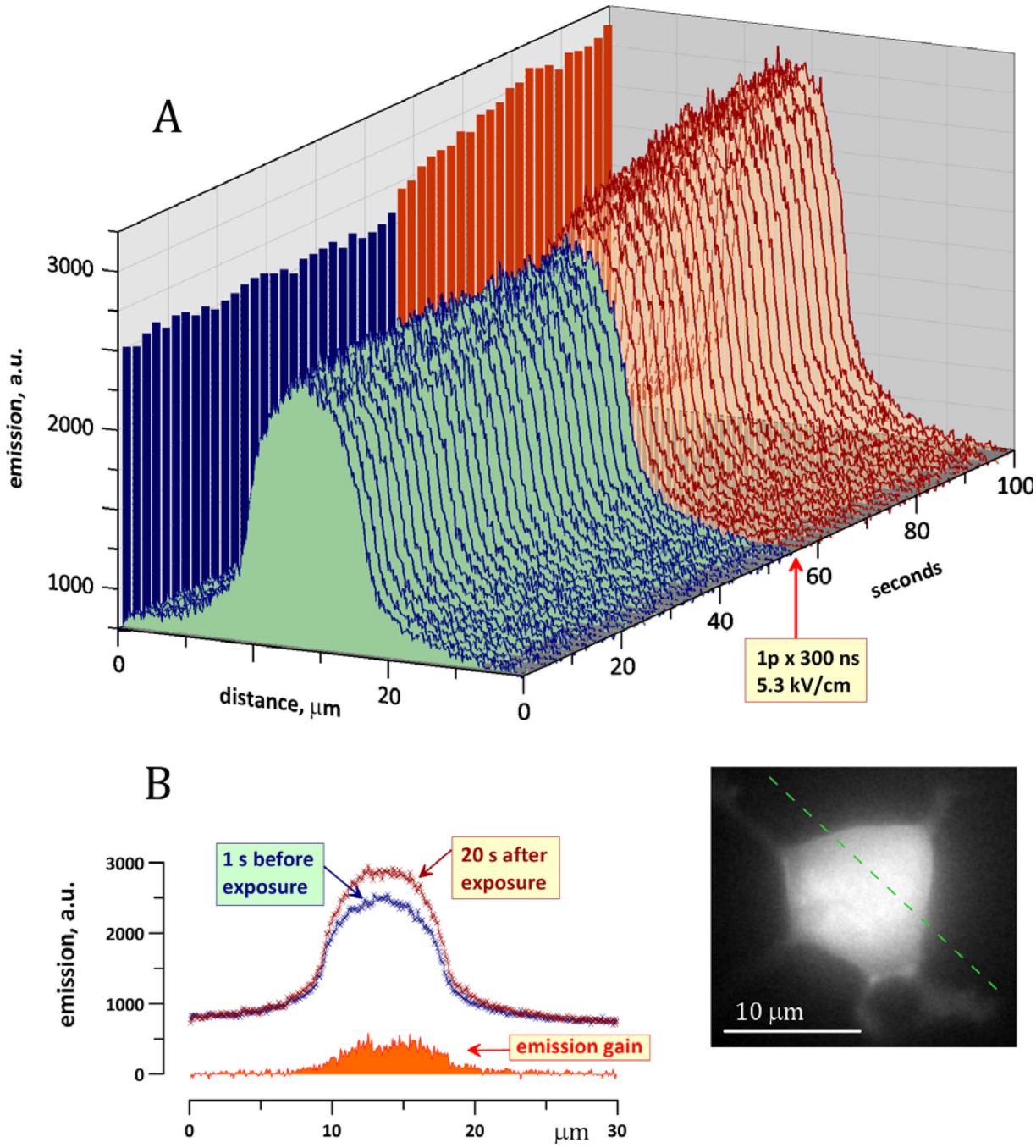

Fig. 4.

Lack of localized increase in $[Na]_i$ in the vicinity of the cell plasma membrane following nsPEF exposure. Inset shows a fluorescent image of the cell loaded with 1 μm of Sodium Green. The emission intensity was measured along the dashed line, which connects the tips of nsPEF-delivering electrodes (not shown). **A:** The emission along the line was measured repeatedly before and after exposure to one 300 ns pulse at 5.3 kV/cm (arrow). Increased emission following exposure reflects the Na^+ influx through the membrane. **B:** Individual line scans of the emission intensity immediately prior to exposure and 20 s after. The emission gain due to exposure is the arithmetic difference between these two curves. Note

maximum emission gain above the center of the cell body and lack of any additional peaks close to the plasma membrane. The calibration of dye emission against $[Na]_i$ that was used in Figure 2 does not apply to line scan measurements presented here.

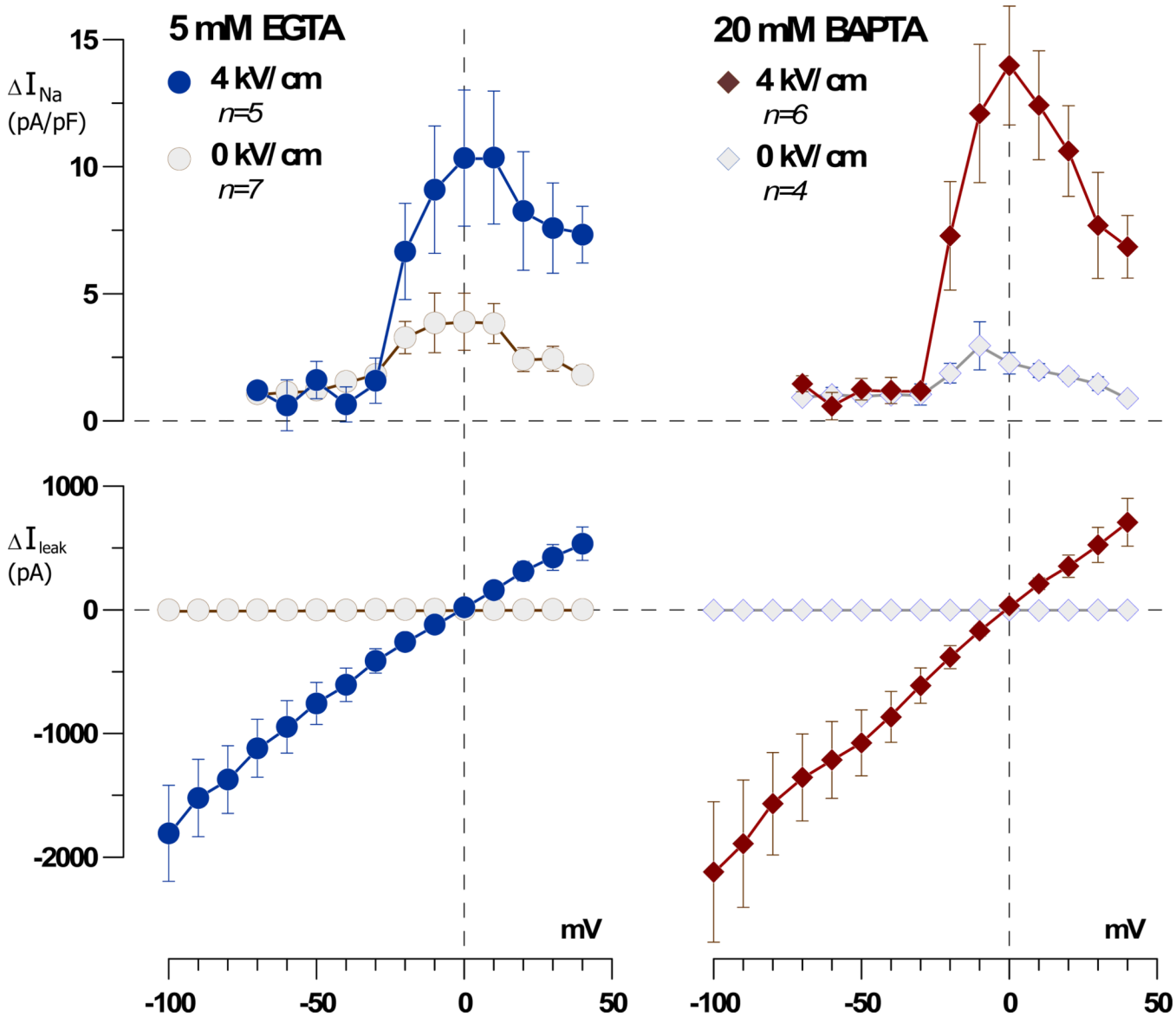

Fig. 5.

High intracellular concentration of a fast Ca^{2+} chelator, BAPTA, does not prevent inhibition of VG I_{Na} by nsPEF. Membrane currents were measured in individual NG108 cells 20 s prior to nsPEF exposure and 30 s after; the former was subtracted from the latter using a "control subtraction" function of the pClamp software. This difference reflected the change in current caused by nsPEF (one 300 ns pulse at 4 kV/cm) or sham exposure. Note that sham-treated cells showed a minor reduction in VG I_{Na} (presumably due to cell rundown) and no change in I_{leak}. The nsPEF-treated cells displayed significantly greater reduction of VG I_{Na} and profound I_{leak}. Adding 20 mM BAPTA instead of 5 mM EGTA into the pipette buffer did not attenuate the nsPEF effects.